Robustness of Median Filter for Suppression of Salt and Pepper Noise (SPN) and Random Valued Impulse Noise (RVIN)

Abdul Rasak Zubair *ar.zubair@ui.edu.ng*
Department of Electrical/Electronic Engineering
University of Ibadan
Ibadan, Nigeria

Hammed Oyebamiji Busari *hammed_busari@yahoo.com*
Department of Electrical/Electronic Engineering
University of Ibadan
Ibadan, Nigeria

Abstract

Noises in images are caused by many sources. Image de-noising has remained an active area of research. Results of numerical experiments on the robustness of median filter for suppression of Salt and Pepper Noise (SPN) and Random Valued Impulse Noise (RVIN) of varying noise densities are presented and discussed. Varying densities of SPN and RVIN were simulated and used to corrupt five selected test images which have different image frequencies. The corrupted images were filtered with Median Filters which has 3 by 3 kernel size. The effects of larger kernels were also examined. The performance metrics are the Peak Signal to Noise Ratio (PSNR) and Gain. SPN is found to have more adverse effects on images than RVIN. However, the Median filter is found to achieve a higher degree of noise suppression with SPN than RVIN. Effects of SPN and RVIN increase with an increase in noise density. Median filtering of SPN and RVIN corrupted images are found to be satisfactory with 3 by 3 kernel for noise densities up to the maximum of 60% and 40% noise densities respectively. Median filter Gain is found to increase with noise density up 40% and then reduce with further increase in noise density. To some extent, there is some correlation between Median filter gain and test image frequency. Using 5 by 5 kernel may improve noise suppression but the resulting filter image is blurred. 3 by 3 is the optimum kernel size.

Keywords: Image Noise, Noise Density, Image Frequency, Median Filter, Peak Signal To Noise Ratio.

1. INTRODUCTION

Images are acquired by devices such as scanners, digital camera, microscope, scanning electron microscope, Charged Coupled Devices (CCD) array, and video camera [1,2,3,4]. An imaging device usually consists of an input source of energy. The principal energy source for images in use today is the electromagnetic energy spectrum. Other important sources of energy include acoustic, ultrasonic, and electronic (in the form of electron beams used in electron microscopy).

The reflected or refracted wave from each point on the object being imaged is detected by a sensor and converted to an electric signal that is further processed and digitized. Charge Couple Device often serves as the transducer. Examples of reflection based systems include Digital Camera and Ultrasound Imaging System. Examples of refraction based systems include x-ray, Magnetic Resonance Imaging System (MRI) and microscopy.

Images like other types of signals are affected by the systems used to acquire, transmit, or process them [1,2,3,4,5]. Sometimes, these systems are imperfect and introduce noise, η, as illustrated in Fig. 1(a) and as described in Eqn. (1). f and g may be gray level images (2-D) or colour images (3-D) with three colour components. Furthermore, the conditions under which signals are acquired are frequently less than ideal. These non-ideal conditions also introduce noise, distortion, or other artifacts.

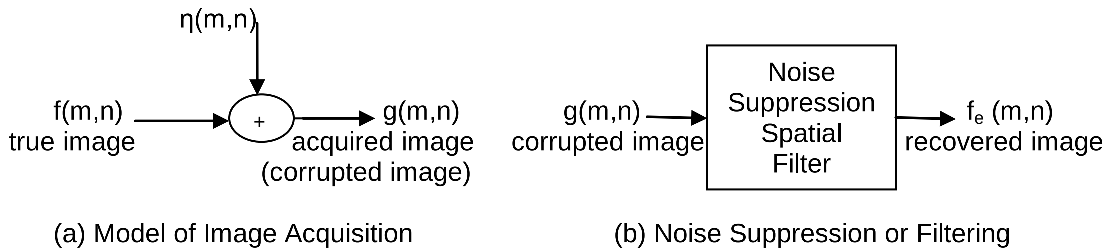

FIGURE 1: Models of Image Acquisition and Noise Suppression or Filtering.

$$g(m,n) = f(m,n) + \eta(m,n) \qquad (1)$$

Noises in images are caused by many sources [6,7,8,9,10,11]. These include atmospheric inhomogeneity in terms of density, temperature and refractive index; spontaneous motion and material inhomogeneity of tissues or organs being imaged; fluctuation in heat, temperature, and infrared radiation; defects in charge coupled devices.

There is the need for the recovery of the true image from the available or acquired image or noisy image, g. Image processing filters are used to suppress either the high frequencies in the image to smooth the image or the low frequencies in the image to enhance or detect edges in the image. Image de-noising has remained an active area of research [12,13,14,15,16].

The available corrupted image g is sent as input to a spatial filter to obtain an output f_e which is an estimate of the true image f as illustrated in Fig. 1(b). A function of values of g in a predefined neighborhood of (m,n) is used to determine the value of f_e at (m,n) as described by Eqn. (2) [1,2,3,4,6]. The filter function h(m,n) is known as the kernel. The kernel is usually a square matrix with size 3 by 3 or 5 by 5 or 7 by 7 or 9 by 9. Differently sized kernels containing different patterns of numbers give rise to different results under convolution [1,2,3,4,6,17,18,19].

$$f_e(m,n) = g(m,n) \otimes h(m,n) \qquad (2)$$

The median filter is normally used to reduce noise in an image like the mean filter [1,2,3,4,5,6,20,21,22,23,24,25,26,27,28,29]. However, median filter preserves useful detail in the image, unlike the mean filter. It replaces every pixel value with the median of neighboring pixel values. The median filter has two main advantages over the mean filter. The median filter is a more robust average than the mean filter and so a single very unrepresentative pixel in a neighborhood will not affect the median value significantly. Since the median value must actually be the value of one of the pixels in the neighborhood, the median filter does not create new unrealistic pixel values when the filter straddles an edge. For this reason, the median filter is much better at preserving sharp edges than the mean filter.

In this work, the robustness of median filter for suppression of Impulse noise is investigated. Impulse noise can be classified mainly into two categories; Salt and Pepper Noise (SPN) and Random Valued Impulse Noise (RVIN). The median filter's performance dependency on the noisy density and a characteristic of the test image known as image frequency are also studied.

2. METHODS

2.1 Noise Simulation

2.1.1 Salt and Pepper Noise (SPN)

Salt-and-pepper noise (SPN) is a form of fixed valued impulse noise. It presents itself as randomly occurring white and black pixels. SPN models defects in the CCD such that some of the intensity values are either erroneously transmitted as ‘0’ or as ‘255’ while the remaining intensity values are transmitted correctly as described in Eqn. (3) [1,2,3,4,6,8]. The total number of pixels in the input image f is M x N. (1-d) % of these pixels appear correctly in the output image g. each of the d% of these pixels has a color component which erroneously appears in the output image as either ‘0' or ‘255' independent of the true corresponding intensity values in the input image f. d is given by Eqn. (4) and is known as noise density. NCP as given by Eqn. (4) is the number of corrupted image pixels. The locations Y of the noisy pixels are randomly selected using the Matlab code "randi". Y is a 1 by NCP matrix containing the 1-D addresses of the noisy pixels [30]. NCP is approximated to the nearest lower whole number; for example, 23.7 is rounded up to 23. Matlab code “floor” is used to achieve this approximation [30]. X is a 2 by NCP matrix containing the 2-D addresses of the noisy pixels.1-D addresses in Y is converted to 2-D addresses in X as described by Eqns. (6) to (9).

$$\mathrm{g}(m,n) = \begin{cases} f(m,n) & \\ \eta & \text{where } \eta \in [0, 255] \end{cases} \tag{3}$$

$$d = \frac{Number\ of\ Corrupted\ Pixels\ (NCP)}{Total\ Number\ of\ Pixels\ (M \times N)} \text{ x } 100\% \tag{4}$$

$$NCP = \frac{dMN}{100} \tag{5}$$

$$\mathrm{Y(y)} \rightarrow X(x_1, x_2) \tag{6}$$

$$\frac{y}{M} = y_1 \text{ remainder } y_2 \tag{7}$$

where y_1 and y_2 are integers.

$$x_2 = \begin{cases} y_1 + 1 & \text{if } \mathrm{y}_2 \neq 0 \\ y_1 & \text{if } \mathrm{y}_2 = 0 \end{cases} \tag{8}$$

$$x_1 = \begin{cases} y_2 & \text{if } \mathrm{y}_2 \neq 0 \\ M & \text{if } \mathrm{y}_2 = 0 \end{cases} \tag{9}$$

2.1.2 Random Valued Impulse Noise (RVIN)

Random valued impulse noise (RVIN) is also known as uniform noise. In random value impulse noise, a noisy pixel can be such that a colour component randomly takes any value from the interval {0,255} [7,9,10,11]. Here, the spectrum of noise is much wider than the fixed value impulse noise. As a result, detection and suppression of random valued impulse noise is a challenging task. The total number of pixels in the input image f is M x N. (1-d) % of these pixels appear correctly in the output image g. Each of the d% of these pixels is such that a colour component randomly and erroneously appears in the output image as any digit between ‘0' and ‘255' independent of the true corresponding intensity value in the input image f. Eqn. (10) describes RVIN.

$$g(m,n) = \begin{cases} f(m,n) & \\ \eta & \text{where } \eta \in [0,1,2,...,254,255] \end{cases} \quad (10)$$

Based on Eqns. (3) to (10), SPN and RVIN are simulated. The flow charts of the simulation algorithms for SPN and RVIN are presented in Fig. (2) and Fig. (3) respectively.

2.2 Median Filter

The median of the values of g in a predefined neighborhood of (m,n) is used as the value of f_e (m,n) [6]. Based on Eqns. (2), a median filtering algorithm is developed.

2.3 Performance Metrics

The Peak Signal to Noise Ratio (PSNR) is a measure of the degree of corruption or degradation of an image with noise or/and blurring [6,31,32]. Eqn. (11) evaluates $PSNR_c$ which compares the corrupted image g with the true image f and Eqn. (12) evaluates $PSNR_r$ which compares the filtered or recovered image f_e with the true image f. Subtracting $PSNR_c$ from $PSNR_r$ gives the Gain as in Eqn. (13). Higher Gain indicates a higher degree of noise suppression by the filter. A negative Gain indicates that the filter adds more noise to the corrupted image instead of suppressing the noise in the image.

$$PSNR_c = 10\log_{10}\left[\frac{255^2}{\frac{1}{3NM}\left[\sum_{m=1}^{M}\sum_{n=1}^{N}\sum_{t=1}^{3}\left(g(m,n,t) - f(m,n,t)\right)^2\right]}\right] \quad (11)$$

$$PSNR_r = 10\log_{10}\left[\frac{255^2}{\frac{1}{3NM}\left[\sum_{m=1}^{M}\sum_{n=1}^{N}\sum_{t=1}^{3}\left(f_e(m,n,t) - f(m,n,t)\right)^2\right]}\right] \quad (12)$$

$$Gain = PSNR_r - PSNR_c \quad (13)$$

The frequency or rate of change of intensity across rows and columns of an image is a characteristic of an image and it often has some effects on the processing of the image. Eqn. (14) gives the frequency estimate of an RGB colour image [6,32].

$$Freq = \frac{1}{3M(N-1)}\frac{\partial I}{\partial j} + \frac{1}{3N(M-1)}\frac{\partial I}{\partial i} \quad (14)$$

where
$$\frac{\partial I}{\partial j} = \sum_{i=1}^{M}\sum_{j=2}^{N}\sum_{t=1}^{3}\left|I(i,j,t) - I(i,j-1,t)\right| \quad (15)$$

and
$$\frac{\partial I}{\partial i} = \sum_{j=1}^{M}\sum_{i=2}^{N}\sum_{t=1}^{3}\left|I(i,j,t) - I(i-1,j,t)\right| \quad (16)$$

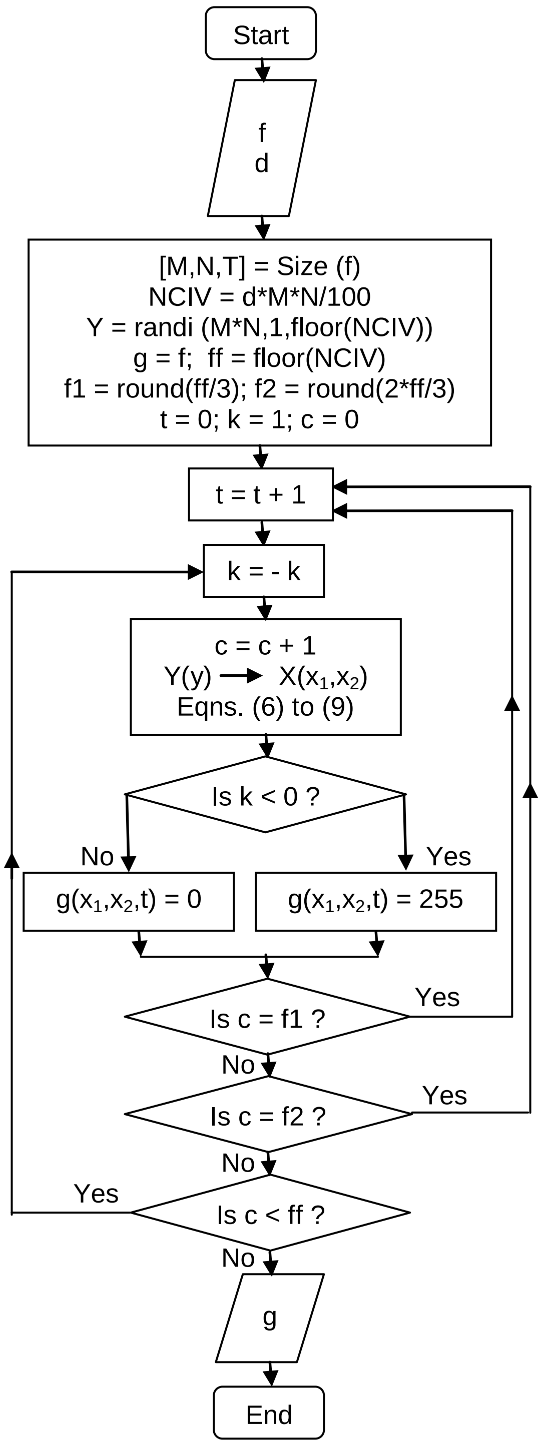

FIGURE 2: Flow Chart for SPN Simulation.

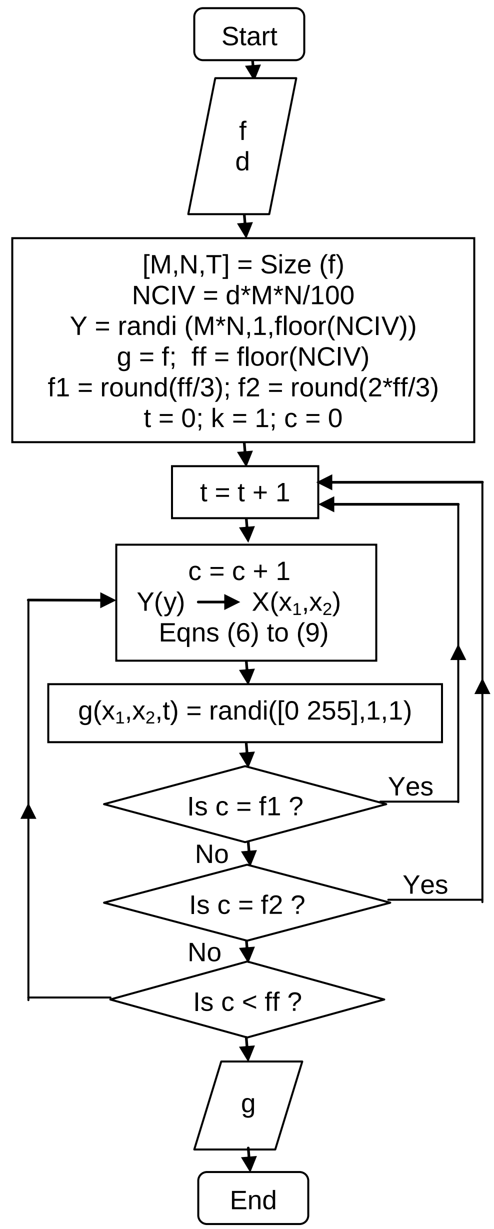

FIGURE 3: Flow Chart for RVIN Simulation.

3. EXPERIMENTAL TESTS, RESULTS AND DISCUSSIONS

3.1 Five Test Images

Five test images [33] are selected to study the robustness of median filter as noise density increases from 5% to 90%. The effect of test image frequency on median filter performance is also investigated.

3.2 Experiment on Robustness of Median Filter for SPN Suppression

The five test images were corrupted with simulated Salt and Pepper Noise (SPN) with noise densities 5%, 10%, 15%, 20%, 40%, 50%, 60%, 70% and 90%. The corrupted images were filtered with Median Filter. A 3 x 3 kernel was used. The frequency of the test images, $PSNR_c$, $PSNR_r$, and Gain were recorded and presented in Table 1 and Fig. 4. Average results for the nine different noise densities are presented in Table 2. Some of the results for two of the five test images are shown in Table 3.

Test Image	Label/ Freq	% Noise density d	5%	10%	15%	20%	40%	50%	60%	70%	90%
	Lena 6.40	$PSNR_c$ (dB)	22.99	20.03	18.30	17.07	14.22	13.33	12.59	11.99	11.05
		$PSNR_r$ (dB)	33.73	33.54	33.34	33.14	31.98	31.08	29.86	28.48	25.74
		Gain (dB)	10.74	13.52	15.04	16.07	17.76	17.75	17.27	16.49	14.70
	Pepper 7.54	$PSNR_c$ (dB)	22.80	19.77	18.03	16.84	13.97	13.07	12.36	11.74	10.79
		$PSNR_r$ (dB)	29.11	29.09	29.12	28.97	28.49	28.01	27.36	26.58	24.41
		Gain (dB)	6.30	9.33	11.09	12.13	14.53	14.93	15.00	14.84	13.62
	House 8.08	$PSNR_c$ (dB)	22.90	19.95	18.22	17.03	14.15	13.25	12.53	11.93	10.97
		$PSNR_r$ (dB)	27.21	27.19	27.11	27.11	26.59	26.16	25.66	25.03	23.34
		Gain (dB)	4.31	7.24	8.89	10.08	12.44	12.92	13.13	13.10	12.37
	Boat 10.62	$PSNR_c$ (dB)	22.74	19.78	18.01	16.81	13.97	13.06	12.35	11.74	10.79
		$PSNR_r$ (dB)	27.41	27.36	27.23	27.14	26.60	26.20	25.65	25.03	23.17
		Gain (dB)	4.67	7.58	9.22	10.34	12.63	13.14	13.30	13.28	12.38
	Baboon 18.76	$PSNR_c$ (dB)	23.04	20.09	18.36	17.15	14.28	13.36	12.67	12.07	11.11
		$PSNR_r$ (dB)	22.74	22.67	22.59	22.51	22.13	21.90	21.64	21.26	20.43
		Gain (dB)	-0.31	2.58	4.23	5.36	7.84	8.54	8.97	9.19	9.32

TABLE 1: Results of Experiment on Robustness of Median Filter for SPN Suppression.

$PSNR_c$ reduces with increase in noise density indicating that the effect of SPN on images become more severe as density increases. $PSNR_r$ also reduces with increase in noise density. Median filter Gain increases with noise density up to 40% and then reduces with further increase in noise density. To some extent, it can be stated approximately that the higher the test image Freq, the lower the Gain and the lower the $PSNR_r$ as observed in Table 2. There is no correlation between test image Freq and $PSNR_c$. For noise densities up to 60%, the filtered images appear noise free as observed in Table 3. Therefore, Median filtering of SPN corrupted images can be said to be satisfactory for noise densities up to the maximum of 60% noise density.

Test Image Label	Test Image Freq	Averages for 9 different noise densities		
		$PSNR_r$ (dB)	$PSNR_c$ (dB)	Gain (dB)
Lena	6.4	31.21	15.73	15.48
Pepper	7.54	27.91	15.49	12.42
House	8.08	26.16	15.66	10.50
Boat	10.62	26.20	15.47	10.73
Baboon	18.76	21.98	15.79	6.19

TABLE 2: Results of Experiment on Robustness of Median Filter for SPN Suppression: Averages for 9 different noise densities.

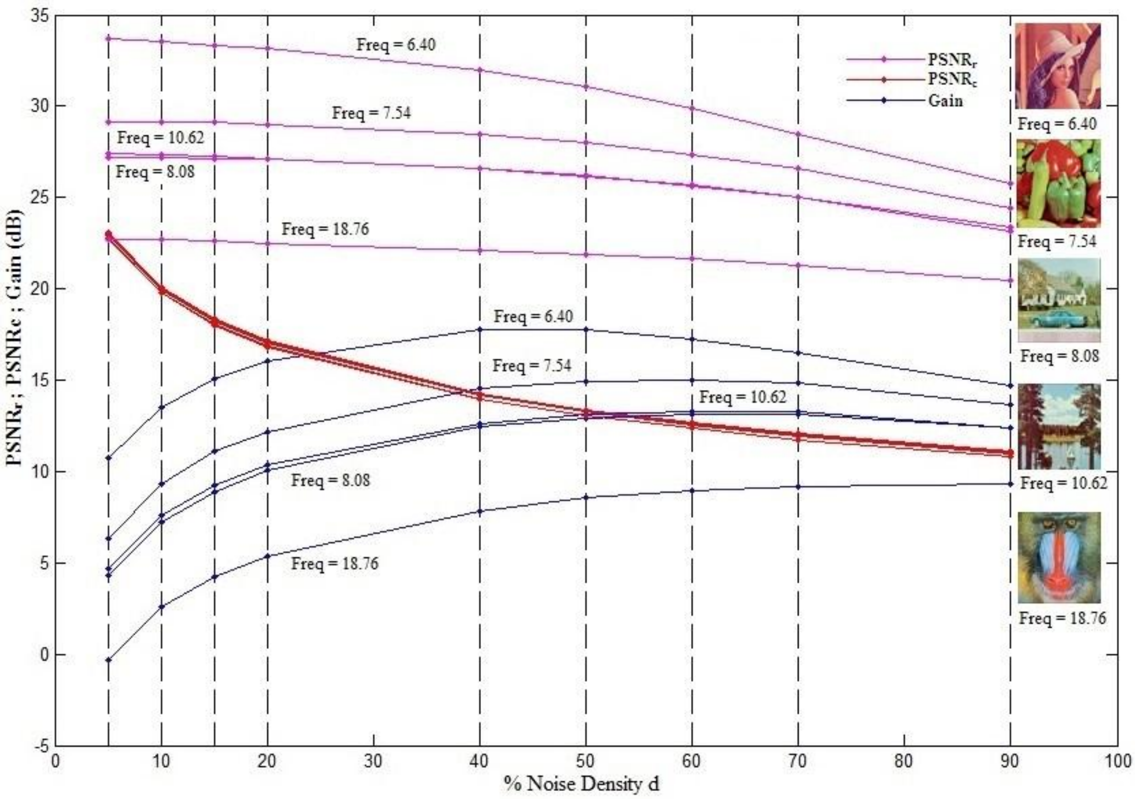

FIGURE 4: Graph of Results of Experiment on Robustness of Median Filter for SPN Suppression.

3.3 Experiment on Robustness of Median Filter for RVIN Suppression

The five test images were corrupted with simulated Random Valued Impulse Noise (RVIN) with noise densities 5%, 10%, 15%, 20%, 40%, 50%, 60%, 70% and 90%. The corrupted images were filtered with Median Filter. A 3 x 3 kernel was used. The frequency of the test images, $PSNR_c$, $PSNR_r$, and Gain were recorded and presented in Table 4 and Fig. 5. Average results for the nine different noise densities are presented in Table 5. Some of the RVIN suppression experimental results for two of the five test images are shown in Table 6.

	Noisy Input Image					
Original Noise Free Image		5% Noise Density PSNRc = 22.99 dB	20% Noise Density PSNRc = 17.07 dB	40% Noise Density PSNRc = 14.22 dB	60% Noise Density PSNRc = 12.59 dB	90% Noise Density PSNRc = 11.05 dB
	Median Filter Output					
		PSNRr = 33.73 dB Gain = 10.74 dB	PSNRr = 33.14 dB Gain = 16.07 dB	PSNRr = 31.98 dB Gain = 17.76 dB	PSNRr = 29.86 dB Gain = 17.27 dB	PSNRr = 25.74 dB Gain = 14.70 dB
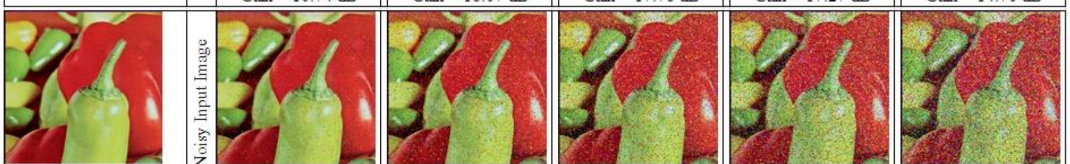	Noisy Input Image					
Original Noise Free Image		5% Noise Density PSNRc = 22.80 dB	20% Noise Density PSNRc = 16.84 dB	40% Noise Density PSNRc = 13.97 dB	60% Noise Density PSNRc = 12.36 dB	90% Noise Density PSNRc = 10.79 dB
	Median Filter Output					
		PSNRr = 29.11 dB Gain = 6.30 dB	PSNRr = 28.97 dB Gain = 12.13 dB	PSNRr = 28.49 dB Gain = 14.53 dB	PSNRr = 27.36 dB Gain = 15.00 dB	PSNRr = 24.41 dB Gain = 13.62 dB

TABLE 3: Experiment on Robustness of Median Filter for SPN Suppression; a case study of two test images.

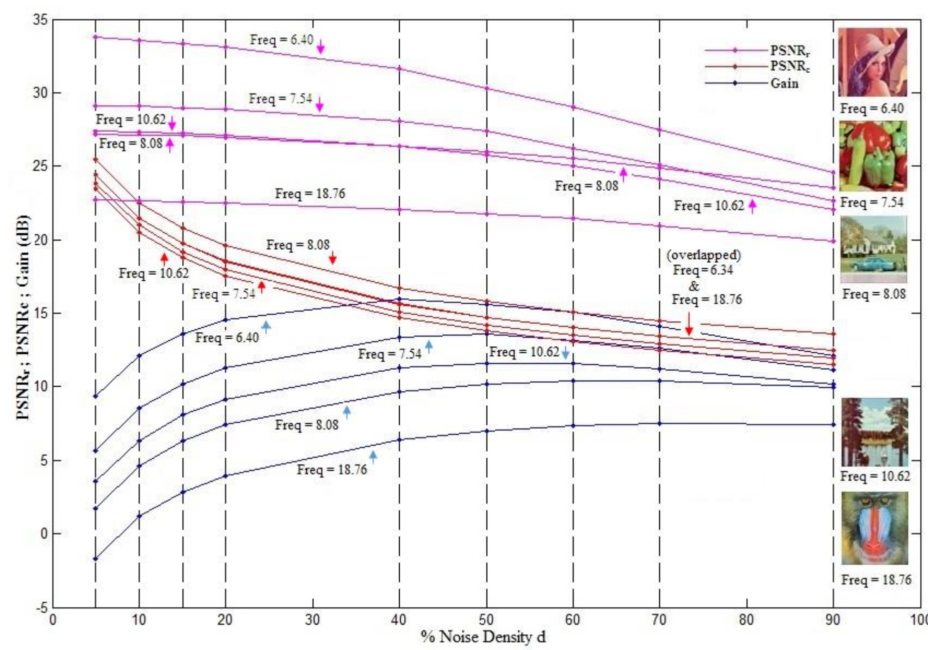

FIGURE 5: Graph of Results of Experiment on Robustness of Median Filter for RVIN Suppression.

Test Image	Label/ Freq	% Noise density d	5%	10%	15%	20%	40%	50%	60%	70%	90%
	Lena 6.40	$PSNR_c$ (dB)	24.42	21.42	19.72	18.49	15.63	14.72	14.01	13.41	12.46
		$PSNR_r$ (dB)	33.75	33.54	33.30	33.08	31.60	30.30	29.05	27.50	24.54
		Gain (dB)	9.33	12.12	13.58	14.59	15.96	15.58	15.04	14.09	12.09
	Pepper 7.54	$PSNR_c$ (dB)	23.46	20.52	18.76	17.55	14.70	13.79	13.05	12.47	11.53
		$PSNR_r$ (dB)	29.12	29.07	28.97	28.86	28.05	27.37	26.21	25.08	22.64
		Gain (dB)	5.66	8.54	10.20	11.31	13.35	13.58	13.16	12.62	11.11
	House 8.08	$PSNR_c$ (dB)	25.50	22.52	20.79	19.58	16.72	15.83	15.09	14.48	13.57
		$PSNR_r$ (dB)	27.19	27.13	27.08	26.98	26.38	25.98	25.52	24.88	23.52
		Gain (dB)	1.69	4.61	6.29	7.40	9.66	10.15	10.43	10.40	9.95
	Boat 10.62	$PSNR_c$ (dB)	23.85	20.98	19.18	17.95	15.11	14.21	13.50	12.89	11.94
		$PSNR_r$ (dB)	27.42	27.31	27.25	27.09	26.39	25.78	25.05	24.15	22.08
		Gain (dB)	3.56	6.33	8.07	9.14	11.27	11.56	11.55	11.25	10.14
	Baboon 18.76	$PSNR_c$ (dB)	24.43	21.44	19.74	18.55	15.65	14.74	14.06	13.43	12.49
		$PSNR_r$ (dB)	22.73	22.66	22.57	22.50	22.04	21.74	21.43	20.94	19.93
		Gain (dB)	-1.70	1.22	2.83	3.95	6.39	7.00	7.37	7.50	7.44

TABLE 4: Results of Experiment on Robustness of Median Filter for RVIN Suppression.

Test Image Label	Test Image Freq	Averages for 9 different noise densities		
		$PSNR_r$ (dB)	$PSNR_c$ (dB)	Gain (dB)
Lena	6.4	30.74	17.14	13.60
Pepper	7.54	27.26	16.20	11.06
House	8.08	26.07	18.23	7.84
Boat	10.62	25.83	16.62	9.21
Baboon	18.76	21.84	17.17	4.67

TABLE 5: Results of Experiment on Robustness of Median Filter for RVIN Suppression: Averages for 9 different noise densities.

$PSNR_c$ reduces with increase in noise density indicating that the effect of RVIN on images become more severe as density increases. $PSNR_r$ also reduces with increase in noise density. Median filter Gain increases with noise density up to 40% and then reduces with further increase in noise density. To some extent, it can be stated approximately that the higher the test image Freq, the lower the Gain and the lower the $PSNR_r$ as observed in Table 5. There is no correlation between test image Freq and $PSNR_c$. For noise densities up to 40%, the filtered images appear noise free as observed in Table 6. Therefore, Median filtering of RVIN corrupted images can be said to be satisfactory for noise densities up to the maximum of 40%.

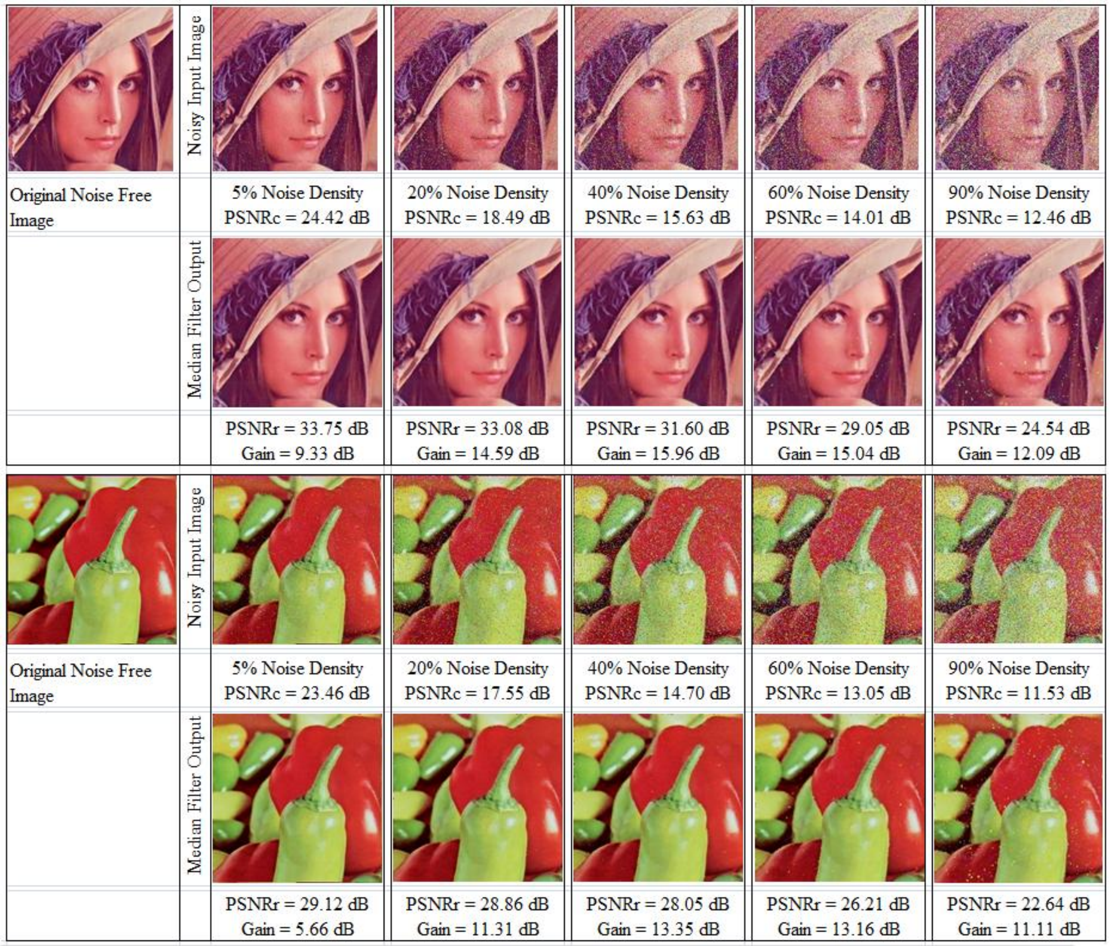

TABLE 6: Experiment on Robustness of Median Filter for RVIN Suppression: a case study of two test images.

3.4 Comparison of The Effect and Suppression of SPN and RVIN

Experimental results for SPN and RVIN are plotted on the same graph for each test image. The graphs for the five test images are placed side by side as shown in Fig. 6. It's observed that $PSNR_c$ of RVIN corrupted image is higher than that for SPN corrupted image for the five test images. Therefore, SPN has more adverse effect on images than RVIN. It's also observed that $PSNR_r$ and median filter gain for SPN suppression are greater than those for RVIN suppression for the five test images. Therefore, median filter achieves a higher degree of noise suppression with SPN than RVIN.

3.5 Effect of Kernel Size On Noise Suppression

An SPN corrupted image with d = 90% was filtered with for different kernel sizes of 3 by 3, 5 by 5, 7 by 7 and 9 by 9. This was repeated for RVIN corrupted image with d = 60%. The results are presented in Table 7 and Fig. 7. Some of the results for two of the five test images are shown in Table 8. As observed in Table 7 and Fig. 7, Gain increased when kernel size was increased from 3 by 3 to 5 by 5 for SPN in all cases but for RVIN in only two out of five cases. Use of 7 by 7 and 9 by 9 do not improve the Gain in most cases. Observed appearance of filtered images in Table 8 indicates that kernel sizes of 5 by 5, 7 by 7 and 9 by 9 have higher noise suppression capacity compared with 3 by 3 kernel. However, output images of median filters with kernel sizes of 5 by 5, 7 by 7 and 9 by 9 are blurred. 3 by 3 is the optimum kernel size.

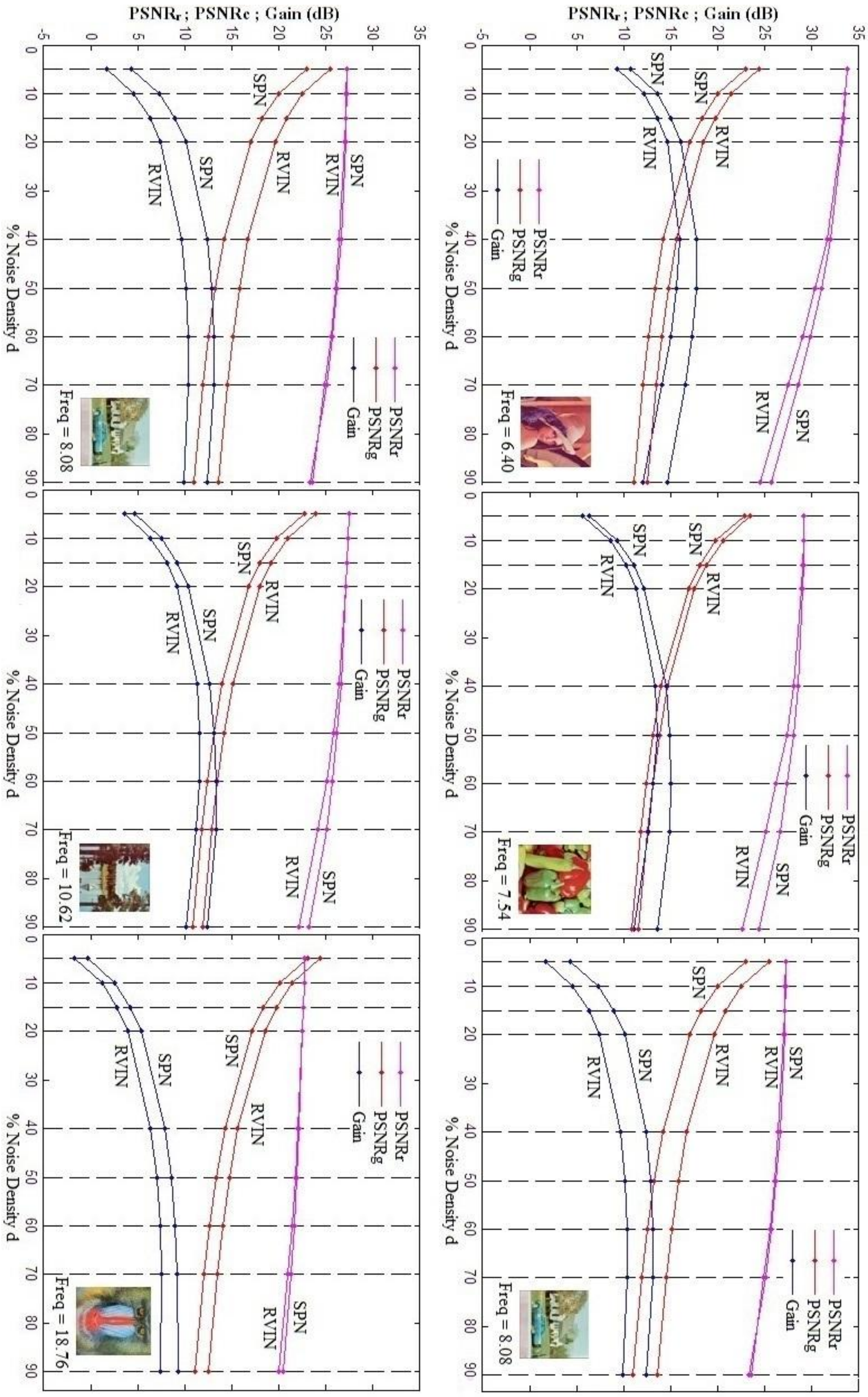

FIGURE 6: Comparison of Results of Experiments on Robustness of Median Filter for RVIN and SPN Suppression for the five test images.

	Test Image	Freq	$PSNR_c$	$PSNR_r$				Gain			
				3 by 3 kernel	5 by 5 kernel	7 by 7 kernel	9 by 9 kernel	3 by 3 kernel	5 by 5 kernel	7 by 7 kernel	9 by 9 kernel
SPN Suppression (d=90%)	Lena	6.4	11.05	25.74	29.38	28.16	27.21	14.70	18.34	17.11	16.17
	Pepper	7.54	10.79	24.41	27.26	26.73	26.07	13.62	16.47	15.94	15.28
	House	8.08	10.97	23.34	24.24	22.97	22.25	12.37	13.27	12.00	11.28
	Boat	10.62	10.79	23.17	24.51	23.35	22.41	12.38	13.72	12.56	11.62
	Baboon	18.76	11.11	20.43	20.24	19.79	19.51	9.32	9.13	8.68	8.41

	Test Image	Freq	$PSNR_c$	$PSNR_r$				Gain			
				3 by 3 kernel	5 by 5 kernel	7 by 7 kernel	9 by 9 kernel	3 by 3 kernel	5 by 5 kernel	7 by 7 kernel	9 by 9 kernel
RVIN Suppression (d=60%)	Lena	6.4	14.01	29.05	29.47	28.10	27.06	15.04	15.46	14.09	13.05
	Pepper	7.54	13.05	26.21	27.19	26.43	25.65	13.16	14.13	13.37	12.60
	House	8.08	15.09	25.52	24.19	22.79	22.01	10.43	9.11	7.70	6.93
	Boat	10.62	13.50	25.05	24.61	23.38	22.39	11.55	11.11	9.88	8.88
	Baboon	18.76	14.06	21.43	20.32	19.79	19.48	7.37	6.26	5.73	5.42

TABLE 7: Comparison of median filter kernel sizes.

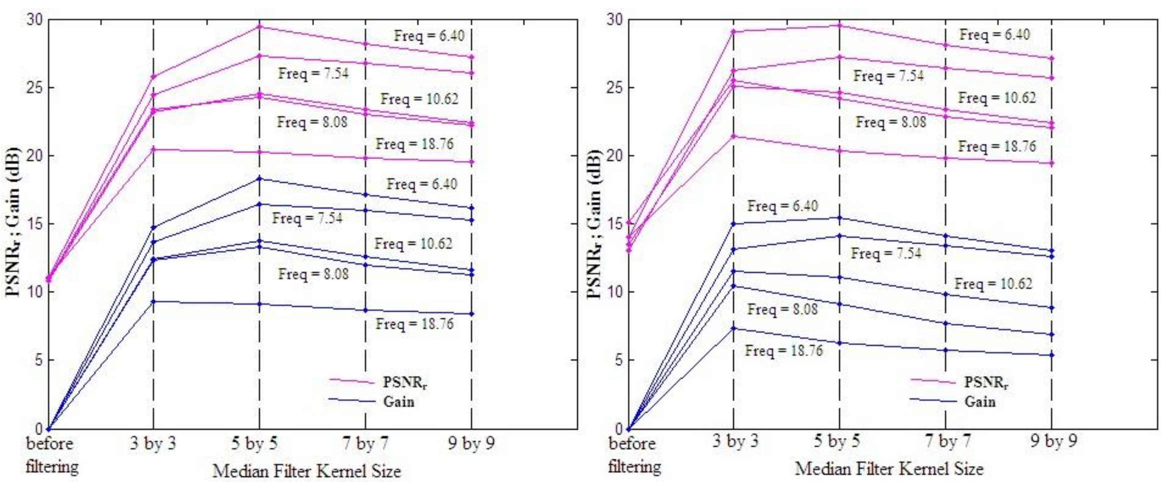

(a) Suppression of SPN with d = 90%   (b) Suppression of RVIN with d = 60%

FIGURE 7: Comparison of Median Filter Kernel Sizes.

3.6 Comparison with Results Obtained In Previous Works

Experimental results obtained in this work compare favourably well with the results obtained in previous works. Table 9 shows that, in most cases, $PSNR_r$ obtained in this work is higher than those obtained in previous works for Lena test image. The details of the rise and fall of the Gain as noise density increases from 0% to 90% was studied and observed in this work; such details are missing in previous works. Like in this work, 3 by 3 is also found to be the optimum kernel size by Shelke & Sharma in [29]. Shelke & Sharma in [29] state that "Larger window has the good noise suppression capability, however, image details (edges, corners, fine lines) preservation is poor; whereas a smaller window preserves the main points however it'll cause the reduction in noise suppression." This agrees with the observation discussed in section 3.5 above.

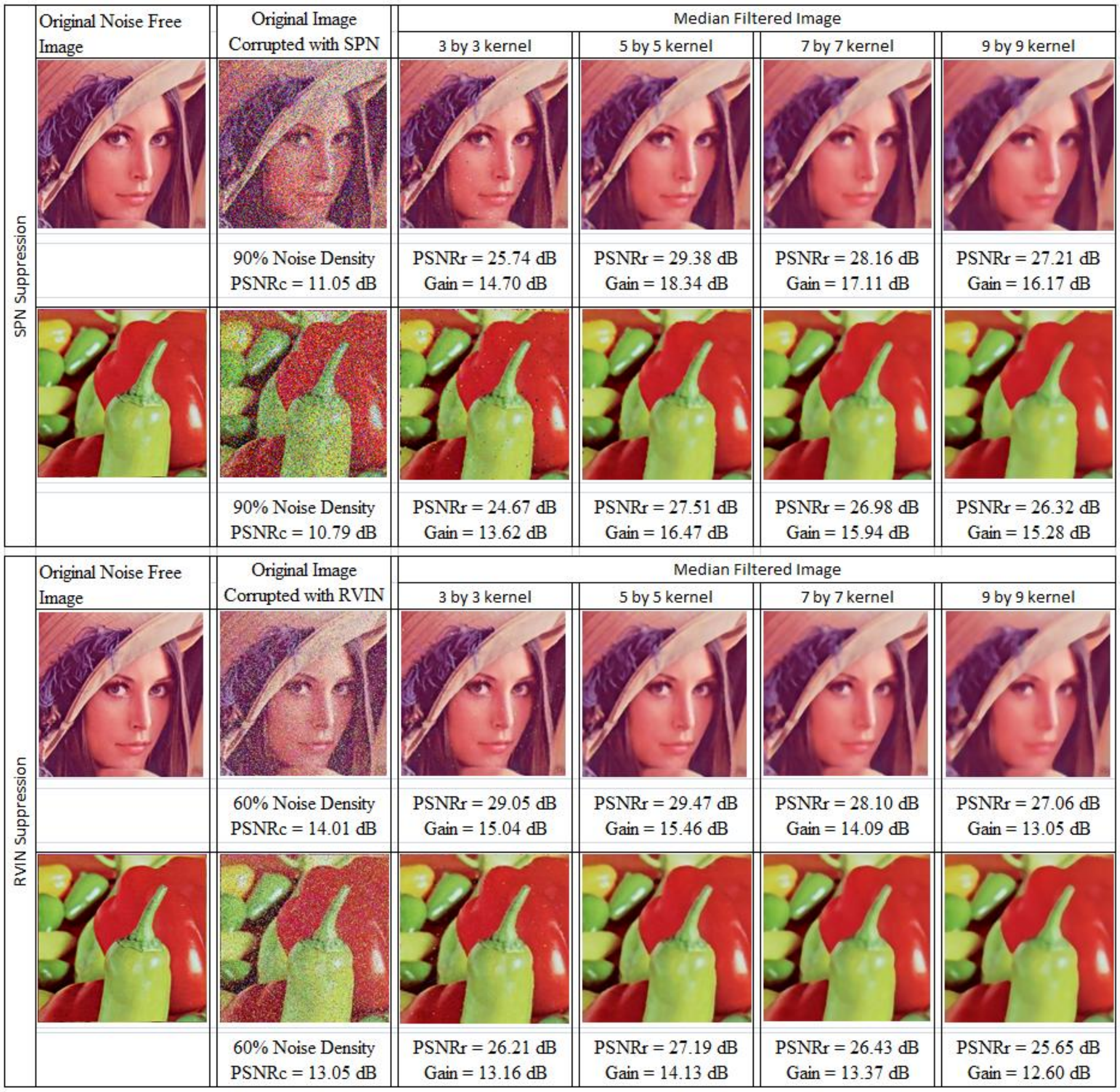

TABLE 8: Comparison of median filter kernel sizes; a case study of two test images.

	% Noise density d	10%	20%	40%	50%	60%	70%	90%
This work	$PSNR_r$ (dB) Zubair & Busari	33.54	33.08	31.60	30.30	29.05	27.50	24.54
Previous works	$PSNR_r$ (dB) Gupta [26]	30.65	29.13	25.04	22.88	19.33	15.82	8.24
	$PSNR_r$ (dB) Sen & Tiwari [27]	28.49	25.75	18.41	14.73	12.24	9.98	6.58
	$PSNR_r$ (dB) Saudia *et. al* [28]	21.98	21.92	21.47	20.65	18.40	14.85	8.06
	$PSNR_r$ (dB) Shelke & Sharma [29]				14.73	13.34	12.60	8.90

TABLE 9: Comparison with results obtained in previous works for Lena test image.

4. CONCLUSION

Simulation of varying densities of Salt and Pepper Noise (SPN) and Random Valued Impulse Noise (RVIN) was implemented based on the characteristics of the types of noise. Five selected test images were corrupted with simulated SPN and RVIN. Median filter with 3 by 3 kernel was used for noise suppression. Median filters with 5 by 5, 7 by 7 and 9 by 9 were also tested. Pick Signal to Noise Ratio (PSNR) and Gain were evaluated. The frequencies of the test images were also computed. Robustness of Median filter for the suppression of the two types of impulse noise has been studied extensively.

SPN has more adverse effect on image Pick Signal to Noise Ratio (PSNR) compared with RVIN. However, the median filter has higher Gain for the suppression of SPN than RVIN. Image Pick Signal to Noise Ratio (PSNR) decreases as noise density increases. Median filter with 3 by 3 kernel is found to be very effective for the suppression of SPN and RVIN for noise densities up to the maximum of 60% and 40% respectively. Median filter Gain increases with noise density up 40% and then reduces with further increase in noise density. There is some correlation between median filter Gain and Image frequency. 5 by 5 kernel may improve noise suppression compared with 3 by 3 kernel but output image resulting from 5 by 5 kernel is blurred. 3 by 3 is, therefore, the best kernel size.

The algorithm developed replaces every pixel value with the median of neighboring pixel values. Future algorithms should be adaptive. Future algorithms should be selective by replacing only pixels that are suspected of being noisy with the median of neighboring pixel values.

5. REFERENCES

[1] B. Chanda and D.D. Majumer. Digital Image Processing and Analysis. India: Prentice-Hall, 2000.

[2] R.C. Gonzalez and R. E. Woods. Digital Image Processing. Massachusetts: Addison-Wesley, 2002.

[3] F.C. Tony and S. Jianhong. Image Processing and Analysis: Variational, PDE, Wavelet, and Stochastic Methods. Philadelphia: SIAM, 2005.

[4] A.K. Jain. Fundamentals of digital image processing. India: Prentice-Hall, 1989.

[5] A. Bovik. Handbook of image and video processing. New York: Academic, 2000.

[6] A.R. Zubair and O.A. Fakolujo. “Development of Statistics and Convolution as Tools for Image Noise.” African Journal of Computing & ICT, vol 6, pp. 53-66, Dec. 2013.

[7] A.S. Ali, and M. Hong. (2007). “Robust Detection Technique for Removing Random-Valued Impulse Noise.” IEEE International Symposium on Signal Processing and Information Technology, 2007, pp. 575-577.

[8] P. Chen and L. Chih-Yuan. “An efficient edge-preserving algorithm for removal of salt-and-pepper noise.” IEEE Signal Processing Letters, vol. 15, pp. 833-836, Dec. 2008.

[9] C. Pinar. "Removal of Random-Valued Impulsive Noise from Corrupted Images." IEEE Transactions on Consumer Electronics, vol. 55, pp. 2097-2104, 2009.

[10] Y. Dong, R.H. Chan and S. Xu, “A detection statistic for random valued impulse noise.” IEEE Trans. Image Process., vol.16, pp. 1112-1120, Apr. 2007.

[11] Y. Dong and S. Xu. “A new directional weighted median filter for removal of random- valued impulse noise.” IEEE Signal Processing Letters, vol. 14, pp.193-196, Mar. 2007.

[12] C. Saxena and D. Kourav. “Noises and Image Denoising Techniques: A Brief Survey.” International Journal of Emerging Technology and Advanced Engineering, vol. 4, no. 3, March 2014) pp. 878-885, Mar. 2014.

[13] A.K. Das. "Review of Image Denoising Techniques." International Journal of Emerging Technology and Advanced Engineering, vol. 4, no. 8, pp. 519-522, Aug. 2014.

[14] L. Hongqiao and W. Shengqian. “A New Image Denoising Method Using Wavelet Transform.” International Forum on Information Technology and Applications, May 2009, pp. 111-114.

[15] K. Gupta and S.K. Gupta. “Image Denoising Techniques – A Review paper.” International Journal of Innovative Technology and Exploring Engineering (IJITEE), vol. 2, no. 4. pp. 6-9, Mar. 2013.

[16] S. Roy, N. Sinha and A.K. Sen. “A New Hybrid Image Denoising Method.” International Journal of Information Technology and Knowledge Management, vol. 2, no. 2, pp. 491-497, 2010.

[17] P. Patidar, M. Gupta, S. Srivastava and A.K. Nagawat. “Image De-noising by Various Filters for Different Noise.” International Journal of Computer Applications, November 2010, vol. 9, no. 4, pp. 45-50, Nov. 2010.

[18] V. Govindaraj and G. Sengottaiyan. “Survey of Image Denoising using Different Filters”, International Journal of Science, Engineering and Technology Research (IJSETR), vol. 2, no. 2, pp. 344-351, Feb. 2013.

[19] A.B. Hamza and K. Hamid. "Image Denoising: A Nonlinear Robust Statistical Approach." IEEE Trans. Signal Processing, vol. 49, pp. 3045-3054, Dec. 2001.

[20] H. Ibrahim, N.S.P. Kong and T.F. Ng. “Simple adaptive median filter for the removal of impulse noise from highly corrupted images.” IEEE Trans. on Consumer Electronics, vol. 54, no. 4, pp. 1920 - 1927, Nov. 2008.

[21] V. Jayaraj and D. Ebenezer. "Anew switching based median filtering scheme and algorithm for removal of high density salt and pepper noise in images." EURASIP Journal on Advances in Signal Processing vol. 2010, pp. 1-11, June 2010.

[22] R. Yang, L. Yin, M. Gabbouj, J. Astola and Y. Neuvo. “Optimal weighted median filters under structural constraints.” IEEE Trans. Signal Processing, vol. 43, pp. 591–604, Mar. 1995.

[23] A.B. Hamza, P. Luque, J. Martinez, and R. Roman. “Removing noise and preserving details with relaxed median filters.” J. Math. Imag. Vision, vol. 11, no. 2, pp. 161–177, Oct. 1999.

[24] G.R. Arce and J.L. Paredes, ‘‘Image Enhancement and Analysis with Weighted Medians.’’ Nonlinear Image Processing (S. Mitra and G. Sicuranza, eds. London: Academic Press), pp. 27-67, 2000.

[25] G. Duncan and G. Beresford. "Median filter behavior with seismic data." Geophysical Prospecting, vol. 43, no. 3, pp. 329-345, Apr. 1995.

[26] G. Gupta, ‘‘Algorithm for Image Processing Using Improved Median Filter and Comparison of Mean, Median and Improved Median Filter.’’ International Journal of Soft Computing and Engineering (IJSCE), vol. 1, no. 5, pp. 304-311, Nov. 2011.

[27] D. Sen and N. Tiwari, ‘‘Edge Preservation with Noise Reduction in Arthritis Image.’’ International Journal for Scientific Research & Development, vol. 2, no. 12, pp. 371-375, 2015.

[28] S. Saudia, J. Varghese, K. Nallaperumal, S.P. Mathew, A.J. Robin and S. Kavitha, "Salt & pepper impulse detection and median based regularization using Adaptive Median Filter." IEEE Region 10 Annual International Conference (TENCON), 2008, pp. 1-6.

[29] N. Shelke and S. Sharma, ''Comparative performance analysis of removal of impulse noise using different Methods." International Journal of Engineering and Computer Science, vol. 4, no. 4, pp. 11553-11557, April 2015.

[30] MathWorks (Matlab). ''Documentation for MathWorks products.'' http://www.mathworks.com/access/helpdesk/help/helpdesk.shtml [Jan. 1, 2009].

[31] S.S.O. Choy, Y. Chan and W. Siu ''An Improved Quantitative Measure of Image Restoration Quality.'' Proc. IEEE International Conference on Acoustics, Speech and Signal Processing (ICASSP'96), 1996, vol. III, pp 1613-1616.

[32] A.R. Zubair, O.A. Fakolujo and P.K. Rajan. (2009, May). "Digital watermarking of still images with color digital watermarks." In IEEE EUROCON, 2009, pp. 1338-1345.

[33] USC-SIPI Image Database. "Standard Test Images.'' http://sipi.usc.edu/database/index.html [Oct. 5, 2006].